

Unveiling Hydrothermal Synthesis and Captivating Characteristics of Nickel Nanoferrites

Amrutesh Kannolli*, Avinash P†, Suvidha P Hegde†

Abstract

Nickel nano ferrite was effectively synthesized utilizing the hydrothermal method, followed by a comprehensive analysis of its characteristics. X-ray Diffraction (XRD) analyses established the average crystallite size to be 34.10 nm. The existence of iron oxide and the formation of nano ferrites were confirmed by Fourier Transform Infrared (FTIR) spectroscopy, which displays absorption peaks at 573 cm¹ and 481 cm¹ in. Scanning Electron Microscopy (SEM) displayed an average particle size of around 80 nm, while Ultraviolet-Visible (UV-Vis) spectroscopy determined a direct band gap energy of 1.5 eV. These results emphasize the extraordinary nanoscale and optical properties associated with the synthesized nickel nano ferrite, and can be used in the field of storage devices, catalysts for chemical processes and in semiconductor applications.

Keywords: Nano ferrite, Hydrothermal method, XRD, FTIR, SEM.

Introduction

The prefix "nano" denotes something very small, at the scale of nanometers (nm), in the field of nanotechnology. We come across an intriguing group of materials with unusual properties resulting from their nanoscale size when we investigate nano ferrites [1]. Ferrites are compounds composed of iron oxide and other metal ions, which may have magnetic properties. Nickel, which has the atomic number 28 and is a transition metal, is a flexible element that is frequently employed in a variety of fields, including electronics and catalysis [2]. The compound NiFe $_2O_4$ represents nickel ferrite as a ferrite material that contains nickel and iron oxide. The cubic spinel structure of this compound contains nickel ions, which occupy tetrahedral

^{*} Department of Physics, Rai Technology University, Bangalore; amrutesh508@ gmail.com

[†] Avinash P 1, Department of Studies in Physics, Vijayanagara Sri Krishnadevaraya University, Ballari; avinashp@vskub.ac.in, suvvisuvidhahegde@gmail.com

positions, and iron ions, which occupy octahedral positions. Whereas the Nickel nano ferrite (Nnf) particles fall within the array of 1 to 100 nm [3]. Nnf can be synthesized by several synthesis procedures, like as the solgel method [4], auto-combustion method [5], co-precipitation method [6], microwave method [7], microemulsion method [8], and the hydrothermal method [9]. As one of these, hydrothermal synthesis is peculiar and effective. Nanoparticle formation may be facilitated by hydrothermal synthesis, in which superheated pressurized water is employed.

The hydrothermal synthesis method stands out as the most effective technique because it generates nanoparticles through water treatment under high temperature and high-pressure conditions. This results in several benefits, including enhanced crystallinity and purity and exact control of particle dimensions and shapes [10].

The benefits of the hydrothermal method (as discussed in Table 1) are that, depending on the required properties, it allows synthesis of nickel nanoferrites with the desired set of customized parameters. The expected advantages of the synthesis approach are uniform particle size distribution, good magnetic properties, and high catalytic activity [11]. The hydrothermal method also provides the capability for doping and surface modification to enhance the performance of nickel nanoferrites in different applications as well [12].

Table 1: Importance of the Hydrothermal Method

Sl. No.	Reference	Significance and Advantages of the Hydrothermal Method.	
1	Mohan et al. (2012) [1]	The research team achieved uniform carbon nanosphere synthesis through controlled reactions under basic conditions.	
2	Mulla et al. (2018) [2]	The authors showed that low-temperature- processed copper sulfide through a hydrothermal synthesis route shows excellent thermoelectric performance.	
3	Sivakumar et al. (2011) [3]	The authors prepared nickel ferrite nanoparticles with controlled crystallinity and particle size for magnetic applications.	
4	Naji et al. (2024) [4]	The present investigation presents hydrothermal synthesis as a cost-effective technique for the fabrication of ferrite nanostructures compared to the sputtered-based process.	
5	Sridhar et al. (2012) [5]	Pure phased, homogeneous, and highly crystalline ferrites have been accomplished by the hydrothermal route as compared to the citrate gel synthesis technique	
6	Nejati et al. (2012) [6]	The authors used a hydrothermal approach to produce nickel ferrite nanoparticles with high magnetisation and uniform structure.	

7	Udhaya et al. (2022) [7]	Copper ferrite nanoparticles prepared via the green synthesis route under hydrothermal conditions demonstrated higher crystallinity and improved photocatalytic activity.
8	Mulud et al. (2020) [8]	A process was reported for the preparation of copper ferrite nanoparticles with a narrow size distribution and structural stability.
9		The researchers used the hydrothermal synthesis method to create copper nanoferrite, which confirmed greater photocatalytic activity for dye degradation.
10	Özçelik (2023) [10]	The authors have synthesised the copper nano ferrite through the hydrothermal method, hence it provides good results in all characterizations, like as in optical and magnetic properties, as well as photocatalytic activity and biocompatibility.

3. Procedures and materials

3.1. Materials

The chemicals used in this particular experiment are liquor ammonia AR grade (NH $_3$) 98%, double-distilled water, ferric nitrate nanohydrate (Fe(NO $_3$) $_3$ 9H $_2$ O) 98% Extra Pure, and nickel nitrate hexahydrate (Ni(NO $_3$) $_2$ 6H $_2$ O) 98% Extra Pure. The supplier of the chemicals was SD-fine Chem Ltd.

3.2. Method

Fe(NO₃)₃ 9H₂O and Ni(NO₃)₂ 6H₂O are dissolved to start the synthesis of nickel nanoferrites in 20 milliliters of distilled water in a 2:1 mole ratio. To ensure homogeneity, the solutions are combined and thoroughly mixed for two hours using a magnetic stirrer. After being transferred to a tightly sealed autoclave, the precursor solution is heated to a temperature of approximately 240°C for three hours. These temperatures and pressures promote the nucleation and growth of nanoparticles [13]. Once the reaction is complete, the autoclave is cooled, and the nanoparticles produced are quenched. The process is then centrifuged for 20 minutes and filtered. We then recover the nickel nanoferrite by centrifuging and filtration, followed by collecting and drying the filtered compound at a high temperature of about 800 °C in a muffle furnace. Nanoparticles synthesized using these methods are then characterized using advanced techniques, including XRD, FTIR, SEM, and UV-Vis spectroscopy to determine their structure and properties in great detail [14].

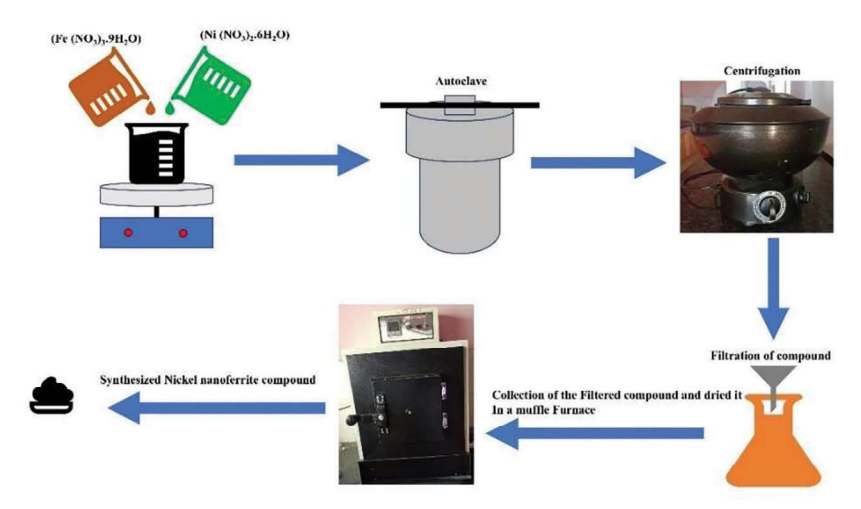


Figure 1: Semantic diagram of the synthesis of nickel nanoferrite using the Hydrothermal method

3.3. Characterization methods used

The diffractograms of the nickel nanoferrite particles were recorded using an X-ray diffractometer with a wavelength of 1.5406 Å. A scanning electron microscope (Carl Zeiss Germany, EVO MA-15) was used to observe the surface morphology. A Fourier infrared spectrophotometer, which operates in the 4000–400 cm⁻¹ range, was used to identify metal ions and functional groups. The Shimadzu (UV-1800) UV-visible instrument is used to find the absorption spectra in the present study.

4. Analysis of results and discussion

4.1. X-ray diffractometer analysis

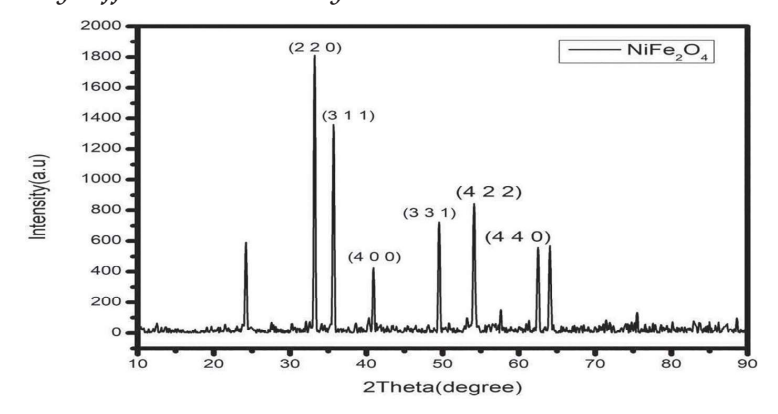


Figure 2: XRD Pattern of NiFe,O₄

The powder XRD pattern of the prepared and annealed sample is shown in the figure. Figure shows that a prepared sample with broad peaks is observed and shows the spinel phase with a cubic crystalline structure. The XRD pattern of the annealed sample exhibits 2θ values such as 24.20° , 33.20° , 35.69° , 40.92° , 49.53° , 54.12° and 62.51° for these 2θ values, the corresponding hkl values (220), (311), (400), (331), (422) and (440) Accordingly, the match with JCPDS card No 00-003-0875 confirms this.

$$D = \frac{0.94\lambda}{\beta\cos\theta} \tag{1}$$

Where the equation (1) is the Debye Scherrer's formula, whereas the D denotes the average crystallite size and β is the peak's full width at half-maxima (FWHM) hence using this formula calculated crystalline size (D) for the above respective peaks from 24.20° to 62.51° the values are 33.07, 34.02, 34.08, 35.39, 34.64, 31.49, and 35.01 average crystalline size is 34.10 nm [15,16].

4.2An analysis of Fourier Transform Infrared Spectroscopy (FTIR):

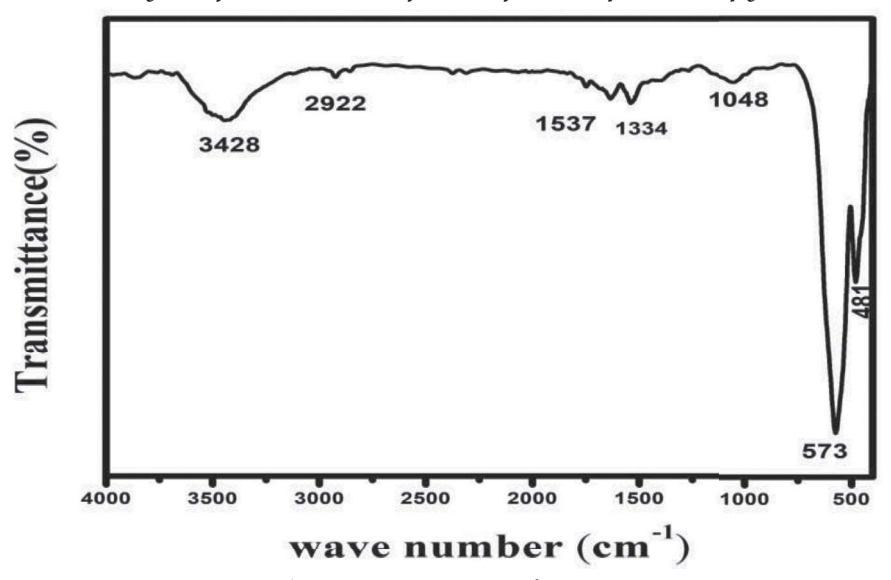


Figure 3: FTIR Pattern of NiFe₂O₄

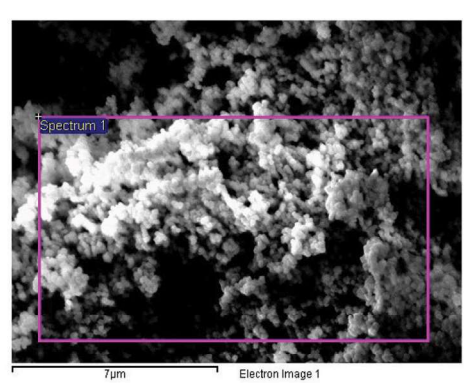
The spectrum reveals a significant band around 3428 cm⁻¹, which describes the stretching modes of the O-H group and indicates the absorbed water or surface Hydroxyl groups. The peak located at 2922 cm⁻¹ is due to C-H stretching vibrations of carboxylic acids [17]. The peak at 1334 cm⁻¹ is

attributed to the C=O stretching vibrations of amides. The peak at 1537 cm⁻¹ results from the bending mode of water molecules [18]. The peak at 1048 cm⁻¹ is due to C-F stretching vibrations associated with alkyl and aryl halides [19]. There are two peaks at 573 cm⁻¹ and 480 cm⁻¹ attributed to C-I stretching vibrations, which correspond to the presence of metal oxide compounds. This is followed by Ni- O or Fe-O vibrations at tetrahedral sites, and at 480 cm⁻¹ by Ni-O or Fe-O vibrations at octahedral sites. [20] The below table shows all the disussed data.

no	Wave number in cm ⁻¹	Functional Group	Description
1	3428	(O-H) stretching	absorbed water or surface
			Hydroxyl groups
2	2922	(C-H) stretching	carboxylic acids
3	1334	(C=O) stretching	vibrations of amides
4	1537	(H-O-H)	bending mode of water molecules
		Bending	
5	1048	(C-F) stretching	vibrations associated with alkyl and
			aryl halides
6	573	Metal-oxygen stretching,	by Ni-O or Fe-O vibrations at
		tetrahedral site	tetrahedral sites
7	480	Metal-oxygen stretching,	by Ni-O or Fe-O vibrations at
		octahedral site	octahedral sites.

Table 2. FTIR wave number analyzed data discussion

4.3. Scanning Electron Microscopy (SEM) Analysis



0 2 4 6 8 10 12 14 16 18
Full Scale 3388 cts Cursor: 0.000

Figure 5: Elemental analysis of

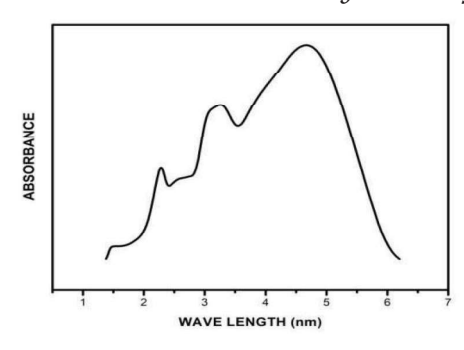
 $NiFe_2O_4$

Figure 4: SEM image of NiFe₂O₄

An image captured by a Scanning Electron Microscope depicts the NiFe₂O₄ sample as shown in Figure 4. The figure illustrates the unusual shape, suggesting the presence of atypical aggregation patterns. From the EDX

spectra (Figure 5), we can identify the elements that are present in this synthesized compound, which are Ni, Fe, and O. This figure demonstrates significant changes in the microstructure. The synthesized powder contains an aggregation of particles that measure less than 100 nm and confirm the crystalline structure of nickel ferrite, which is also indicated by the XRD profile. ImageJ software analysis confirmed that the average particle size of NiFe₂O₄ was 80 nm [21].

4.4. The UV - Visible analysis is as follows:



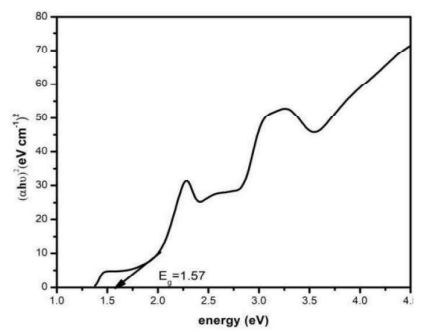


Figure 6: absorption spectra in the UVvisible range of the synthesized NiFe₂O₄ compound

Figure 7: NiFe₂O₄ compound with a direct band gap

The measurement of the direct band gap is a crucial aspect of research in semiconductors and nanomaterials. For insulating substances, the energy of the direct band gap is generally very high (more than 4 eV), which prevents electron movement from the valence band to the conduction band, making the material non-conductive [22]. On the other hand, semiconductors showcase notably lower direct band gap energies, facilitating electron transitions and conductive characteristics that are crucial for various uses. The direct band gap of the synthesized nickel nano ferrite was found to be 1.57 eV utilizing UV-Visible spectroscopy, underscoring its potential usefulness in semiconductor related technologies [23]. The band gap energy was computed using the standard equation developed from Tauc's plot analysis [24].

$$hv = \frac{1240}{wavelength(nm)} \tag{2}$$

$$\alpha h \upsilon = (2.303 \times absorbance \times energy)^2$$
 (3)

The absorption coefficient is symbolized by the character " α ," while Planck's constant is indicated by the letter "h. " The frequency is symbolized by "v," the energy bandgap is symbolized by "Eg," and for the direct case, the value of "n" is presumed to be 2. the space between bands [25].

5. Conclusion

The hydrothermal process was used to effectively manufacture nickel nano ferrite, and its characteristics were comprehensively examined. The XRD analysis revealed an average crystallite size of 34.10 nm, while FTIR investigations confirmed the existence of iron oxide and the production of nanoferrites, which had unique absorption peaks at 573 cm⁻¹ and 481 cm⁻¹. An average particle size of around 80 nm was found by SEM examination, and a direct band gap of 1.5 eV was found by UV-Visible spectroscopy. According to these findings, nickel nano ferrite produces enhanced optical properties and better nanoscale characteristics, making it useful for semiconductor applications.

Acknowledgement

The authors would like to thank Rai Technology University, Bangalore, for the facilities and support provided, that is required to take up this research work.

Funding Statement

This study was not supported by any grant from public, commercial or non-profit funding agencies. The costs of this study were covered by the authors individually.

Contribution of Authors

Dr. Avinash Pandurang: Had substantial contributions in manuscript editing and revising, approving the final version to be submitted for publication.

Suvidha Hegde: Synthesized and characterized the samples.

Dr. Amrutesh Kannolli: Carried out the synthesis, characterization, and analytical examinations; subsequently prepared the full range of results; and composed the initial draft of the publication.

Declaration of Interests:

The individuals contributing to this paper state unequivocally that there are no competing interests of any kind regarding its publication.

References

- Mohan AnuN, Manoj B. Synthesis and Characterization of Carbon Nanospheres from Hydrocarbon Soot. International Journal of Electrochemical Science. 2012 Oct 1;7(10):9537–49. https://doi.org/10.1016/s1452-3981(23)16217-1
- 2. Mulla R, Rabinal MHK. Copper sulfides: Earth-Abundant and Low-Cost thermoelectric materials. Energy Technology. 2018 Oct 10;7(7). https://doi.org/10.1002/ente.201800850
- 3. Sivakumar P, Ramesh R, Ramanand A, Ponnusamy S, Muthamizhchelvan C. Synthesis and characterization of nickel ferrite magnetic nanoparticles. Materials Research Bulletin. 2011 Sep 22;46(12):2208–11. https://doi.org/10.1016/j.materresbull.2011.09.009
- Naji NE, Aljubouri AA, Ismail RA. Synthesis and characterization of nickel ferrite nanostructures by DC Reactive sputtering technique using new target configuration. Plasmonics. 2024 Jul 23; https://doi.org/10.1007/s11468-024-02439-6
- Sridhar R, Ravinder D, Kumar KV. Synthesis and characterization of copper Substituted nickel Nano-Ferrites by Citrate-Gel technique. Advances in Materials Physics and Chemistry. 2012 Jan 1;02(03):192-9. https://doi.org/10.4236/ampc.2012.23029
- 6. Nejati K, Zabihi R. Preparation and magnetic properties of nano size nickel ferrite particles using hydrothermal method. Chemistry Central Journal. 2012 Mar 30;6(1). https://doi.org/10.1186/1752-153x-6-23
- 7. Udhaya PA, Ahmad A, Meena M, Queen MAJ, Aravind M, Velusamy P, et al. Copper Ferrite nanoparticles synthesised using a novel green synthesis route: Structural development and photocatalytic activity. Journal of Molecular Structure. 2022 Dec 17;1277:134807. https://doi.org/10.1016/j.molstruc.2022.134807
- 8. Mulud FH, Dahham NA, Waheed IF. Synthesis and characterization of copper ferrite nanoparticles. IOP Conference Series Materials Science and Engineering. 2020 Nov 1;928(7):072125. https://doi.org/10.1088/1757-899x/928/7/072125
- 9. Mazurenko J, Sijo AK, Kaykan L, Kotsyubynsky V, Gondek Ł, Zywczak A, et al. Synthesis and characterization of copper ferrite nanoparticles for efficient photocatalytic degradation of organic dyes. Journal of Nanotechnology. 2025 Jan 1;2025(1). https://doi.org/10.1155/jnt/8899491
- 10. Özçelik S. Copper ferrite nanoparticles: structural, magnetic, optical, photocatalytic activity and blood compatibility properties. BioNanoScience. 2023 May 19;13(3):958–72. https://doi.org/10.1007/s12668-023-01130-0
- 11. Yadav RS, Kuřitka I, Vilcakova J, Havlica J, Masilko J, Kalina L, et al. Structural, dielectric, electrical and magnetic properties of CuFe2O4 nanoparticles synthesized by honey mediated sol-gel combustion method and annealing effect. Journal of Materials Science Materials in Electronics. 2017 Feb 9;28(8):6245–61.https://doi.org/10.1007/s10854-016-6305-4
- 12. Kumar D, Verma R, Chauhan A, Thakur P, Wan F, Thakur A. Sustainable high frequency applications of copper ferrite nanoparticles. Inorganic

- Chemistry Communications. 2025 Jan1;114018. https://doi.org/10.1016/j.inoche.2025.114018
- 13. Hegazy EZ, El-Maksod IHA, Ibrahim AM, El-Shafay SES. New insights about the formation of copper ferrite: in situ X-ray diffraction study. Bulletin of the National Research Center/Bulletin of the National Research Center. 2018 Oct 10;42(1). https://doi.org/10.1186/s42269-018-0010-9
- 14. Haque MdM, Rahman A, Shahin MdSI, Habib MdA, Khan MdAR, Mahiuddin Md, et al. Manganese doped copper ferrite nanoparticles: A promising approach for organic dye elimination under light irradiation. Results in Chemistry. 2024 Jan 1;7:101509. https://doi.org/10.1016/j.rechem.2024.101509
- Surashe VK, Mahale V, Keche AP, Alange RC, Aghav PS, Dorik RG. Structural and electrical properties of copper ferrite (CuFe2O4) NPs. Journal of Physics Conference Series. 2020 Oct 1;1644(1):012025. https://doi.org/10.1088/1742-6596/1644/1/012025
- 16. Faramawy AM, El-Sayed HM. Enhancement of magnetization and optical properties of CuFe2O4/ZnFe2O4 core/shell nanostructure. Scientific Reports. 2024 Mar 23;14(1). https://doi.org/10.1038/s41598-024-57134-7
- 17. Kannolli A, Avinash P. Physicochemical investigation of synthesized bismuth and Silver-Doped bismuth nanoferrites, and their dielectric properties. IOP Conference Series Materials Science and Engineering. 2024 Apr 1;1300(1):012038. https://doi.org/10.1088/1757-899x/1300/1/012038
- Kannolli A, Avinash P, Shettar AK, Hoskeri JH, G KM. A pilot study: Changes of MDAMB-231 cancer cell line response to synthesized oleic acid – coated MgFe2O4 nano ferrite compound and its cytotoxic effects on L929 cell line. Chemical Physics Impact. 2023 Nov 24;7:100396. https://doi.org/10.1016/j.chphi.2023.100396
- Kannolli A, Avinash P, H B. An investigation of the dielectric behavior of Bi0.7La0.3FeO3 compound under the influence of different calcination temperatures. Chemical Physics Impact. 2023 Oct 9;7:100336. https://doi.org/10.1016/j.chphi.2023.100336n
- Kannolli A, Avinash P, Manohara SR, Taj M, MG K. In-depth study of zinc nanoferrite particles at different calcination temperatures and their behavior in the presence of electric and magnetic fields. Journal of Magnetism and Magnetic Materials. 2023 Jul 26;584:171079. https://doi.org/10.1016/j.jmmm.2023.171079
- 21. Dave PN, Thakkar R, Sirach R, Chaturvedi S. Effect of copper ferrite (CuFe2O4) in the thermal decomposition of modified nitrotriazolone. Materials Advances. 2022 Jan 1;3(12):5019- 26. https://doi.org/10.1039/d2ma00250g
- 22. Devsharma SC, Rahman MdL, Hossain MdJ, Biswas B, Ahmed MdF, Sharmin N. Elucidation of structural, electromagnetic, and optical properties of Cu-Mg ferrite nanoparticles. Heliyon. 2024 Jun 25;10(13):e33578. https://doi.org/10.1016/j.heliyon.2024.e33578n
- 23. Kiey S a. A, Ramadan R, El-Masry MM. Synthesis and characterization of mixed ternary transition metal ferrite nanoparticles comprising cobalt,

- copper and binary cobalt- copper for high-performance supercapacitor applications. Applied Physics A. 2022 May 9;128(6).https://doi.org/10.1007/ s00339-022-05590-1
- Mazurenko J, KSA, Kaykan L, Michalik JM, Gondek Ł, Szostak E, et al. Magneto-24. Structural properties of MG-Substituted copper ferrite nanoparticles. Materials Research Express. 2024 Dec 1;11(12):125003. https://doi.org/10.1088/2053-1591/ad9c19
- 25. Noreen S, Hussain A. Structural, optical, morphological and magnetic properties of Cu0.25M0.75Fe2O4 (M=Mn, Mg, Ni and co) ferrites for optoelectronic applications. Optical Materials [Internet]. 2023 Apr 24;139:113797 https://doi.org/10.1016/j.optmat.2023.113797